through superconductivity," *J. Appl. Phys.*, vol. 33, pp. 875–879, Mar. 1962.
[14] R. Berwin, E. Weibe, and P. Dachel, "Superconducting magnet for a Ku-band maser," in *Proc. 1972 Applied Superconductivity Conf.* (Annapolis, MD, May 1–3, 1972), pp. 266–269.
[15] W. H. Higa and E. Weibe, "A simplified approach to heat exchanger construction for cryogenic refrigerators," *Cryogenic Technol.*, vol. 3, pp. 47–48, 50–51, Mar./Apr. 1967.
[16] L. J. Rickard, P. Palmer, M. Morris, B. Zuckerman, and B. E. Turner, "Detection of extragalactic carbon monoxide at millimeter wavelengths," *Astrophys. J.*, vol. 199, pp. L75–L78, July 15, 1975.
[17] W. B. Burton, M. A. Gordon, T. M. Bania, and F. J. Lockman, "The overall distribution of carbon monoxide in the plane of the galaxy," *Astrophys. J.*, vol. 202, pp. 30–49, Nov. 15, 1975.
[18] B. Zuckerman, T. B. H. Kuiper, and E. N. R. Kuiper, "High-velocity gas in the Orion infrared nebula," *Astrophys. J.*, vol. 209, pp. L137–L142, Nov. 1, 1976.
[19] S. Weinreb, "Millimeter wave varactor down converters," presented at the Diode Mixers at Millimeter Wavelengths Workshop, Max-Planck-Institut für Radioastronomie, Bonn, West Germany, Apr. 1977.

Electrical Characterization of Transferred Electron Devices by a Novel Galvanomagnetic Technique

J. McBRETNEY AND M. J. HOWES

Abstract—**A novel technique is described that utilizes a galvanomagnetic phenomenon for the characterization of transferred electron devices. It is shown that this technique offers important advantages over present techniques based on the use of dummy packages and thus represents a useful analytical tool for the optimum design of transferred electron amplifier and oscillator circuits.**

I. Introduction

THE PERFORMANCE of transferred electron devices as microwave oscillators or amplifiers is critically dependent upon the microwave circuit in which they are embedded. Moreover, studies have indicated that the optimization of the microwave circuit (which includes the package) with regard to stability and noise in oscillators [1], [2] and stabilization and amplification characteristics in amplifiers [3], [4] requires a knowledge of the transferred electron device admittance.

The measurement of transferred electron device admittance is, however, complicated by the fact that the device is almost invariably encapsulated in a small package. Direct measurement, therefore, is impossible. Furthermore, at *X*-band frequencies and above, it would be futile to attempt the direct measurement of a "bare" chip since parasitics would seriously affect the measured admittance. An indirect method, therefore, must be adopted.

In this paper existing indirect methods are described briefly, and some of the disadvantages of their use are discussed. A new method based on galvanomagnetic effects is then described which circumvents these difficulties. It is shown that this technique enables the transfer matrix of a two-port network representing the package and mount to be evaluated and, hence, the device admittance found. Results for the admittance of the package and mount are compared with those based on the use of existing methods.

The method has been successfully applied to the characterization of various transferred electron devices having low contact and interfacial resistances.

II. Previous Methods of Device Characterization

Previous techniques for transferred electron device characterization have one feature in common. They require measurements to be made on particular configurations of dummy packages: that is, packages from which the active device has been removed and the internal geometry altered in some way. Two of these techniques will be considered here; the first is applicable to stable device characterization (amplifiers) while the second is applicable only to oscillating device characterization.

Manuscript received March 29, 1978; revised August 22, 1978.

J. McBretney is with the Ministry of Defence, Admiralty Surface Weapons Establishment, Portsdown Cosham, Portsmouth, England.
M. J. Howes is with the Department of Electrical Engineering, University of Leeds, Leeds, England.

0018-9480/79/0300-0256$00.75 ©1979 IEEE

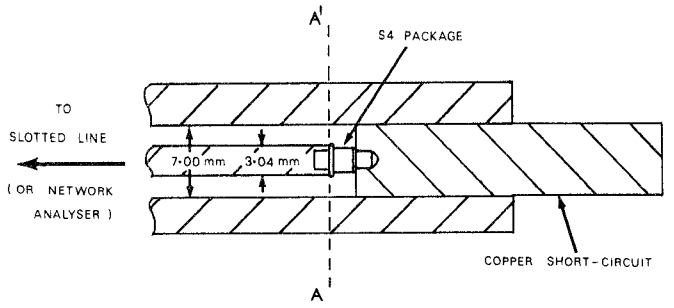

Fig. 1. S4 packaged device in 50-Ω 7-mm coaxial mount.

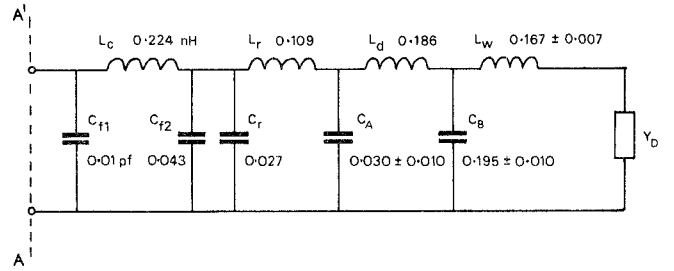

Fig. 2. Lumped-element equivalent circuit of a mounted S4 package, derived by Owens [9].

A. Equivalent Circuit Approach

Considerable effort has been devoted to obtaining a lumped-element equivalent circuit for the device package [3], [5]–[9], since this would enable the device admittance to be computed from a measurement of the encapsulated admittance. In particular, Owens and Cawsey [6], [9] have assumed that the device package (Type S4) was lossless and proceeded as follows. Internally short- and open-circuit dummy packages were first constructed. The former were obtained by bonding a gold wire (from the top contact) directly to the pedestal of the package. The latter were obtained either by 1) bonding a gold wire to a thin n^+ GaAs layer grown on a semi-insulating GaAs substrate mounted on the pedestal, 2) removing the substrate and leaving the gold wire hanging as close to the pedestal as possible without making contact, or 3) bonding the wire directly to a metal contact put down on a semi-insulating GaAs substrate.

The dummy packages were mounted in turn against a short circuit in a 50-Ω 7-mm precision coaxial airline as shown in Fig. 1. The admittance at plane AA' was measured for each package using a slotted line, and these measurements were used to derive a lumped-element equivalent circuit for the mounted package over the desired frequency range. Fig. 2 shows the equivalent circuit derived by Owens [9] in which the values of certain elements, representing the mount ($L_c, L_r, C_{f1}, C_{f2}, C_r$, and L_d), were estimated by calculations based on the work of Getsinger [5], while the remaining element values, representing the package itself, were derived by a process of curve-fitting to the dummy package measurements.

There are, however, at least four factors which are not taken into account in this technique.

1) It is very difficult to construct electrically short- and open-circuit packages at microwave frequencies.

2) Significant spreads exist in the dimensions (and, hence, admittance) of different samples of mass-produced packages.

3) Manufacturers resort to various bonding arrangements including different numbers of wires of various diameters, as well as meshes and tapes. It is important that the exact bonding configuration is known so that it may be repeated in constructing the dummy packages.

4) The manufacturers' bonding processes give rise to a variable and ill-defined structure which cannot be repeated in the dummy packages.

These factors introduce errors and uncertainties which give rise to the derivation of an inaccurate equivalent circuit. In addition, the usefulness of the equivalent circuit is limited by the fact that it is only valid in the circuit configuration of Fig. 1.

B. Approach for Oscillators

A technique for the characterization of oscillating solid-state devices has been described by Howes and Jeremy [10], [11]. An ingenious extension of this technique was developed by Pollard *et al.* [12] in which a 50-Ω tapered coaxial line is taken up inside a dummy package mounted in a waveguide circuit. With the aid of an automatic network analyzer, the admittance looking out into the circuit from the position normally occupied by the device may be measured. After replacing the dummy package arrangement with a packaged device biased to the required operating point, power and frequency measurements are made. The device admittance may then be calculated using the basic equation for stable oscillation given by Kurokawa [1].

This technique has several advantages, but it also suffers from the following disadvantages.

1) It is very difficult to construct a 50-Ω line that tapers from the standard 7-mm diameter connected to the network analyzer, to less than 1 mm inside the package. Any deviation from 50 Ω gives rise to measurement inaccuracies.

2) The geometry of the package is altered because of the need to bore a hole through the pedestal.

3) Comments 2), 3), and 4) of Section II-A apply.

Factor 1) concerns the question of measurement accuracy. The other factors cast doubts over the assumption that the measured admittance is that seen by the device. Hence, the accuracy of the calculated device admittance must be questioned.

III. Proposed Galvanomagnetic Technique

The galvanomagnetic technique presented here [13] is a novel approach to the problem of characterizing transferred electron devices and their microwave circuits. The use of dummy packages is avoided, and thus the difficulties described above are overcome.

The basic technique, which is applicable to the characterization of stable transferred electron devices, is de-

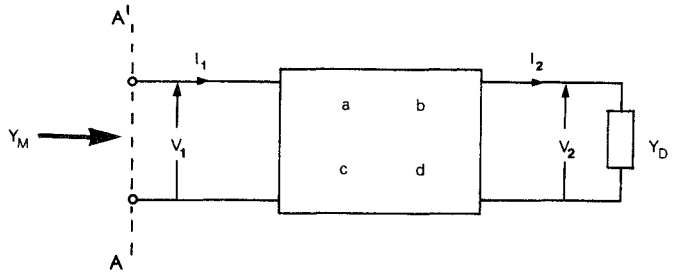

Fig. 3. Equivalent circuit of Fig. 1.

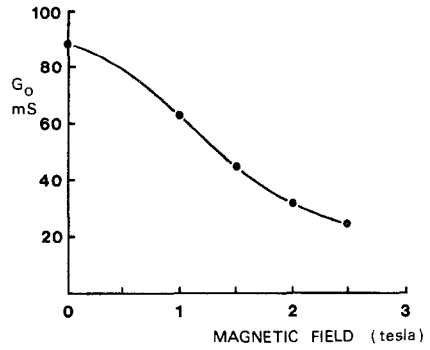

Fig. 4. Typical variation of low-field conductance with transverse magnetic field for an X-band transferred electron device (applied voltage approximately zero).

scribed first. An extension to the basic technique by which oscillating transferred electron devices may be characterized is then considered.

A. Basic Technique—Small-Signal Characterization of Stable Transferred Electron Devices

The packaged device is mounted in a suitable circuit such as that of Fig. 1. This can be represented by a two-port network terminated by the device admittance Y_D as shown in Fig. 3. The voltages and currents are related according to

$$\begin{bmatrix} V_1 \\ I_1 \end{bmatrix} = \begin{bmatrix} a & b \\ c & d \end{bmatrix} \begin{bmatrix} V_2 \\ I_2 \end{bmatrix} \tag{1}$$

where $\begin{bmatrix} a & b \\ c & d \end{bmatrix}$ is the transfer matrix of the two-port network.

From (1) we have

$$\frac{I_1}{V_1} = \frac{cV_2 + dI_2}{aV_2 + bI_2} \tag{2}$$

or

$$Y_M = \frac{c + dY_D}{a + bY_D} \tag{3}$$

where Y_M, the admittance at plane AA', may be measured using a slotted line or, as in this work, using an automatic network analyzer.

Equation (3) may be reduced to

$$Y_M = \frac{C + Y_D}{A + BY_D} \tag{4}$$

where A, B, and C are complex and frequency dependent. It is evident from (4) that, if Y_M can be measured for three known values of Y_D, three equations are obtained which may be solved simultaneously for A, B, and C. Once this has been achieved, it is possible to derive any unknown value of Y_D from a measurement of Y_M. The problem of obtaining three known terminations has been overcome in the present work by using the geometric magnetoresistance effect whereby the application of a transverse magnetic field to a bulk semiconductor of suitable aspect ratio results in a decrease in its low-field conductance G_0. (Most transferred electron devices of practical interest have a suitable aspect ratio.) A typical measurement of low-field conductance against a transverse magnetic field for an X-band device is shown in Fig. 4. It is apparent that a 300-percent change in G_0 is available for a change in magnetic field from 0–2.5 T.

Thus the measurement technique is as follows. With the device unbiased and under the influence of a magnetic field B_1, the admittance at plane AA', Y_{M1} is measured using a network analyzer. The conductance G_{01} pertaining to magnetic field B_1 is measured accurately using a resistance bridge. This procedure is repeated for two other values of G_0 giving, from (4),

$$Y_{M1}(A + B(G_{01} + j\omega C_0)) = C + G_{01} + j\omega C_0 \tag{5}$$

$$Y_{M2}(A + B(G_{02} + j\omega C_0)) = C + G_{02} + j\omega C_0 \tag{6}$$

$$Y_{M3}(A + B(G_{03} + j\omega C_0)) = C + G_{03} + j\omega C_0. \tag{7}$$

These three equations where Y_{M1}, Y_{M2}, Y_{M3}, A, B, C are functions of frequency may be solved simultaneously for A, B, and C at each measurement frequency.

By rearrangement of (4) we have

$$Y_D = \frac{A - BY_M}{CY_M - 1}. \tag{8}$$

Therefore, the device may now be biased to a desired stable operating point via a bias tee (not shown in Fig. 1), and the active device admittance may be calculated from a fourth set of admittance measurements using (8).

The device capacitance C_0 in (5)–(7) is the dielectric capacitance which can be estimated from the electrical parameters of the device

$$C_0 \simeq \frac{\epsilon G_0}{en_0\mu_0} \tag{9}$$

where μ_0 and G_0 are the low-field mobility and conductance, respectively, in the absence of a magnetic field. If C_0 cannot be estimated with sufficient accuracy, then an iterative procedure may be adopted as discussed in Section IV-B.

It should be noted that the galvanomagnetic technique assumes that the low-field conductance is frequency independent. In particular, the low-field conductance is assumed to be the same at dc as at the microwave frequencies of interest. The validity of this assumption is confirmed in Section III-C.

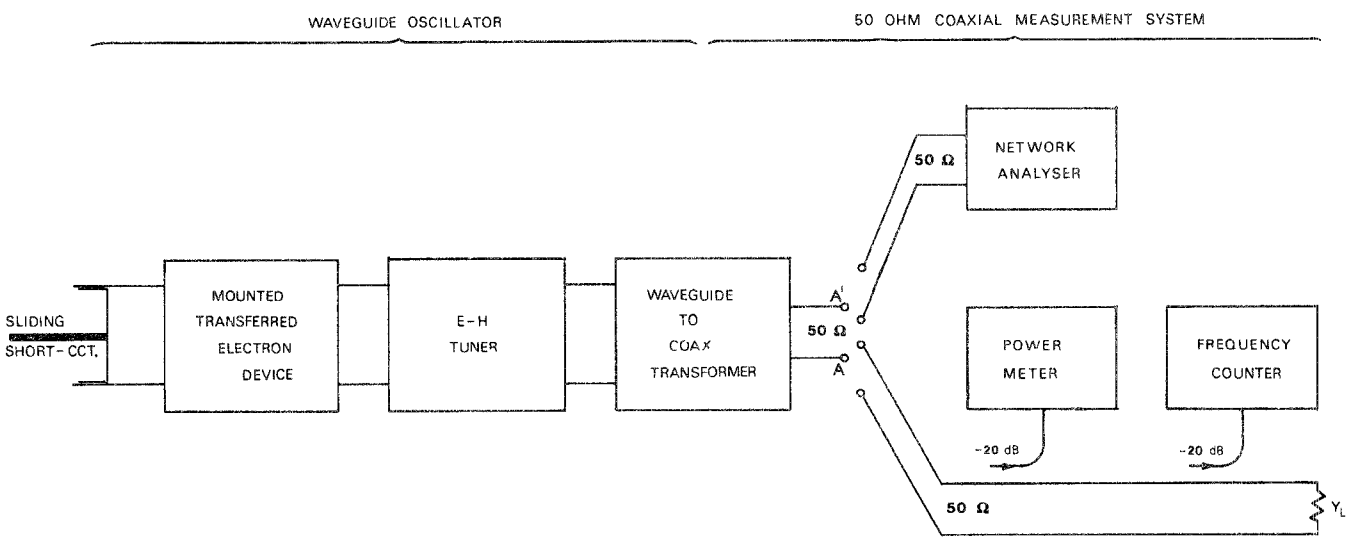

Fig. 5. Schematic diagram of suggested experimental arrangement for characterization of transferred electron oscillators.

B. Characterization of Transferred Electron Oscillators

The basic galvanomagnetic technique may be extended to include characterization of transferred electron oscillators. A schematic diagram of the experimental arrangement is shown in Fig. 5.

It should be noted that, although a waveguide oscillator circuit is indicated, there is no intrinsic objection to a coaxial circuit, nor are the precise details of the circuit arrangement critical. The necessary common feature (satisfied by all practical oscillators) is an output port to which may be attached first a network analyzer, for passive admittance measurements, followed by a matched power and frequency measurement system for active measurements.

The first part of the experimental procedure follows the basic technique described in the preceding section. The network analyzer is connected to port AA' and the admittance Y_M measured for three known values of Y_D obtained, as before, by the application of a transverse magnetic field to the unbiased device. The circuit to the left of AA' may be represented by the equivalent circuit of Fig. 3 except that the two-port network now represents not just the mounted device package but the entire circuit excluding the device. The characteristic parameters (A, B, and C) of this two-port network are computed as before.

The second part of the experiment involves replacing the network analyzer with a matched power and frequency measurement system. The device is then biased to oscillation at some desired operating voltage, and the power and frequency of oscillation are measured.

Now the condition for stable oscillation [1] is that the total admittance at any reference plane should be zero. Therefore, representing the active device admittance by Y_A and the matched measurement system admittance by Y_L (50 Ω), we have at plane AA':

$$\frac{C(\omega_0)+Y_A(V_B,V_{RF},\omega_0)}{A(\omega_0)+B(\omega_0)Y_A(V_B,V_{RF},\omega_0)}+Y_L=0 \qquad (10)$$

from which Y_A may be computed.

If the two-port network is assumed to be lossless, the RF voltage across the device may be deduced from

$$G_A V_{RF}^2+P_L=0 \qquad (11)$$

where P_L is the output power.

In practice, device characterization is usually required over a range of frequencies and power levels for various bias voltage. It is, therefore, more convenient to reverse the order of the experimental procedure. That is, the device is first biased to its required operating point and the microwave circuit (sliding short circuit and EH field tuner) adjusted to give the desired oscillation frequency and power. The matched measurement system is then replaced by the network analyzer, and the circuit is analyzed as before but only at the frequency of interest. Thus only three network analyzer measurements are required. The procedure could be further speeded up by using a precision coaxial switch at port AA'.

C. Consideration of Relaxation and Skin Effects

For the galvanomagnetic technique described above to be applicable, it is essential that the low-field device conductance be frequency independent up to the highest frequency of interest. In this connection, there are two phenomena which must be considered; these are relaxation effects and skin effects.

A numerical analysis of relaxation effects in GaAs has been conducted by Rees [14]. Fig. 6 shows the small-signal frequency dependence of the differential mobility for several bias fields. It can be seen that, as the bias field approaches zero, the frequency dependence of the differential mobility also tends to zero. Therefore, because we are concerned with very small bias fields ($E \ll 10^5 \mathrm{V \cdot m^{-1}}$), we may conclude that relaxation effects are negligible up to at least 150 GHz.

The contribution to the low-field resistance due to the skin effect is rather more difficult to quantify. It depends

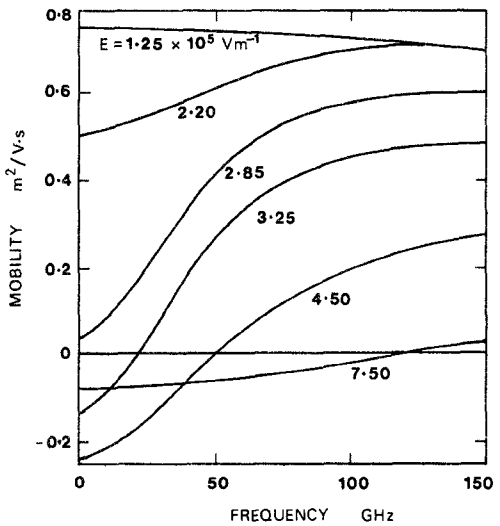

Fig. 6. Frequency dependence of differential mobility in GaAs for several bias fields, after Rees [14].

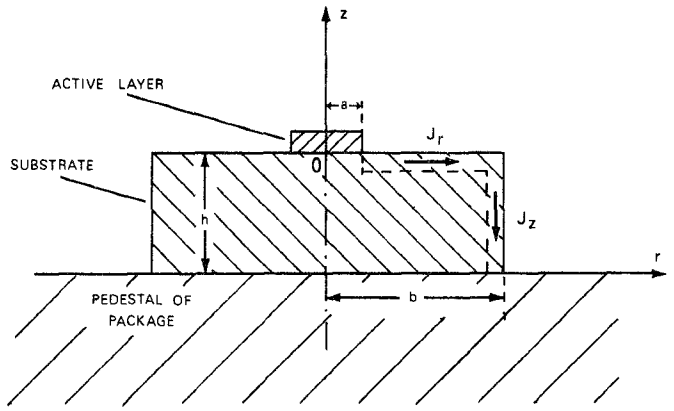

Fig. 7. Simplified cross section of device for calculation of skin effect resistance in the substrate.

on the device geometry and conductivity, and on the frequency of interest. In considering the contribution due to the skin effect, it is convenient to look at the active layer and substrate separately. A typical device might have an active layer thickness of 10^{-5} m and a donor concentration n_0 of 10^{21} m^{-3}, which corresponds to a conductivity σ of 128 $S \cdot m^{-1}$.

Such material has a skin depth of approximately 320×10^{-6} m at 20 GHz. We may deduce from this that the skin effect is negligible in the active layer. The substrate, however, requires more careful consideration because of its higher conductivity, typically of order 10^5 $S \cdot m^{-1}$. The skin depth in material of this conductivity is approximately 10^{-5} m at 20 GHz which is considerably less than the substrate thickness. Because of this, the current will tend to be confined to the surface of the substrate at high frequencies, and this will effect a reduction in substrate conductance.

Although a complete analysis of substrate conductance would involve a difficult numerical computation, it is possible, by making certain simplifying assumptions, to perform an approximate analysis.

A simplified cross section of the substrate (assumed cylindrical) is shown in Fig. 7. Its radius is b and thickness h. The radius of the active layer is a.

In the analysis that follows, it is assumed that the displacement current is negligible ($\sigma \gg \omega\epsilon$), and that the dimensions of the substrate are much greater than the skin depth d (to be defined). Furthermore, it is assumed that the conductivity of the gold-plated pedestal, to which the substrate is bonded, is infinite. This theoretical concept implies that although the current in the pedestal flows in an infinitely thin layer at the surface, the resistance is zero [15].

Current densities in the radial and axial directions within the substrate can be defined as below [16]:

$$J_r = J_0 \frac{a}{r} \exp z(1+j)/d \tag{12}$$

$$J_z = -J_0 \frac{a}{b} \exp (r-b)(1+j)/d \tag{13}$$

where J_0 is the surface current-density at $r=a$, $z=0$, and

$$d = \sqrt{\frac{2}{\omega\mu\sigma}} \ . \tag{14}$$

Now the power dissipated in the radial direction is given approximately by

$$P_1 = \int_a^b \int_0^\infty (|\overline{J_r}|2\pi r)^2/(\sigma 2\pi r) \cdot dz \, dr \tag{15}$$

i.e.,

$$P_1 = \frac{1}{2} \int_a^b \int_0^\infty \frac{1}{\sigma} (J_0 a)^2 \frac{1}{r^2} \exp 2z/d \cdot 2\pi r \cdot dz \, dr \tag{16}$$

$$= \frac{1}{\sigma} (J_0 a)^2 \frac{\pi d}{2} \ln \frac{b}{a}. \tag{17}$$

Similarly, the power dissipated in the axial direction is given approximately by

$$P_2 = \int_{-h}^0 \int_{-\infty}^b (|\overline{J_z}|2\pi b)^2/(\sigma 2\pi b) \cdot dr \, dz \tag{18}$$

i.e.,

$$P_2 = \frac{1}{2} \int_{-h}^0 \int_{-\infty}^b \frac{1}{\sigma} J_0^2 \left(\frac{a}{b}\right)^2 \exp 2(r-b)/d \cdot 2\pi r \cdot dr \, dz \tag{19}$$

$$= \frac{1}{\sigma} (J_0 a)^2 \frac{\pi d}{2} \frac{h}{b}. \tag{20}$$

Now the total rms current is given by

$$I_T = \int_{-\infty}^0 |\overline{J_r}|2\pi r \, dz = J_0 a \sqrt{2} \, \pi d. \tag{21}$$

Therefore, the total power dissipated in the substrate $(P_1 + P_2)$ is given by

$$P = \frac{I_T^2}{\sigma} \frac{1}{4\pi d} \left(\ln \frac{b}{a} + \frac{h}{b}\right). \tag{22}$$

Finally, the substrate resistance P/I_T^2 is

$$R = \frac{1}{4\pi\sigma d} \left(\ln \frac{b}{a} + \frac{h}{b}\right). \tag{23}$$

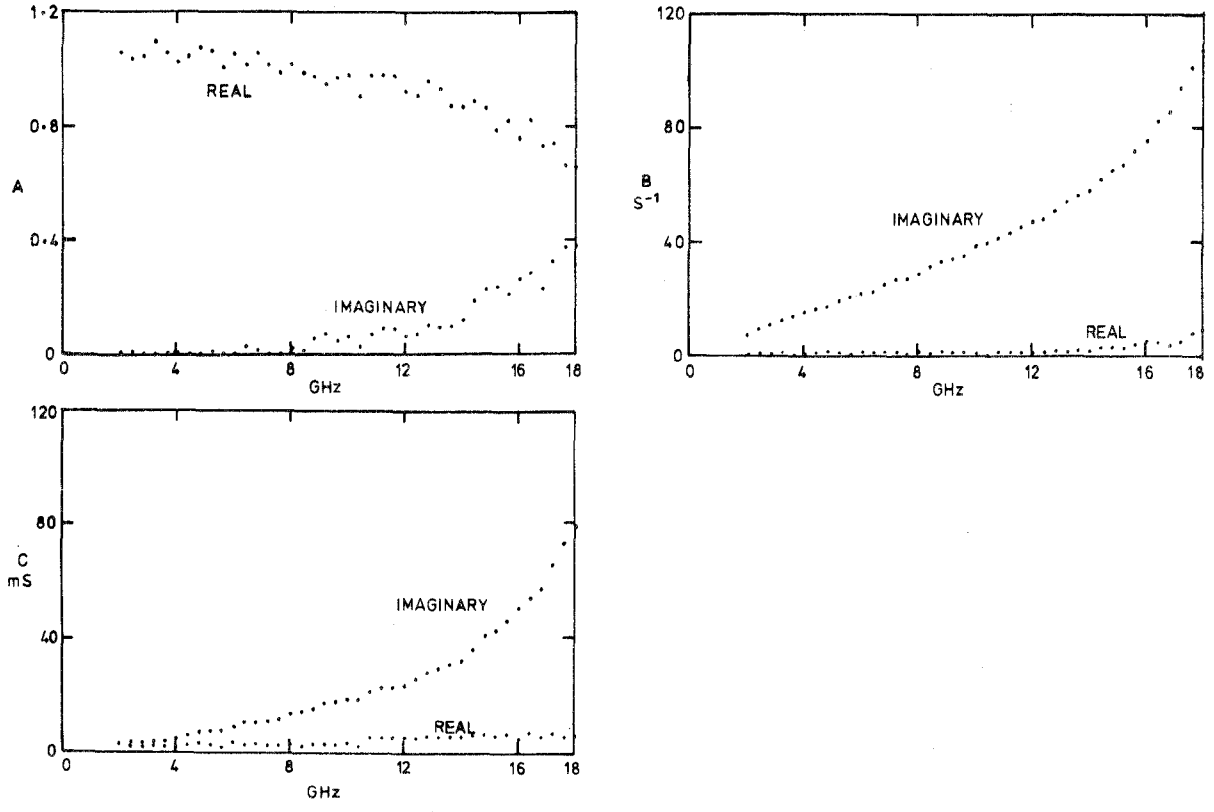

Fig. 8. Package characterization for device number 2400 in 50-Ω coaxial mount of Fig. 1.

For a typical low-power device $\sigma = 10^5$ S·m^{-1}, $b = 100 \times 10^{-6}$ m, $a = 30 \times 10^{-6}$ m, $h = 60 \times 10^{-6}$ m. The skin depth d is 15.9×10^{-6} and 11.3×10^{-6} m at 10 and 20 GHz, respectively.

From (23) the total substrate resistance is

$$R = 0.092\ \Omega \text{ at } 10\text{ GHz}$$

$$R = 0.128\ \Omega \text{ at } 20\text{ GHz}.$$

It is apparent, therefore, that the substrate resistance is approximately two orders of magnitude less than the active layer resistance (approximately 10 Ω for an X-band device) up to 20 GHz.

The advent of improved fabrication techniques such as the integral heat-sink technique [17] has given rise to even thinner and smaller substrates than the example above, and, consequently, the skin effect resistance is further reduced.

It may be concluded from the investigations described above that both relaxation effects and skin effects are negligible, in connection with the requirements of the galvanomagnetic technique, for frequencies up to 20 GHz.

IV. Evaluation of the Galvanomagnetic Technique

In this section, typical package characterization results, obtained using the galvanomagnetic technique, are presented and discussed. A method is then described by which the error associated with the use of the galvanomagnetic technique may be estimated, and a possible correction procedure outlined. Finally, a comparison is made of S4 package admittance measurements obtained using the present technique with those obtained using the previous dummy package technique.

A. Package Characterization Results

Package characterization was carried out using several Plessey devices which were encapsulated in S4 packages. Measurements were made at 200-MHz intervals in the range of 2–18 GHz using a Hewlett–Packard Automatic Network Analyzer set up in the reflection-test mode. Magnetic fields of approximately 0, 1.5, and 2 T were used for the characterization, although the values are not critical provided that a reasonable variation in G_0 is achieved. Measurements were also taken at a magnetic field of approximately 1 T for use in the error estimation procedure discussed in Section IV-B.

Two characterizations (A, B, C) are shown in Figs. 8 and 9. Points are plotted at 400-MHz intervals. The devices, whose identification numbers are 2400 and 1978, are X- and J-band devices, respectively, having nominal maximum power outputs of 100 mW when operated as oscillators. The measured low-field conductance for device number 2400 at 293 K was 87.7, 63.3, 44.6, and 32.3 ms at approximately 0, 1, 1.5, and 2 T, respectively. The corresponding figures for device number 1978 were 114.9, 86.1, 62.1, and 46.1 ms. The zero-bias capacitances of the two devices were estimated at 0.04 and 0.06 pF, respectively.

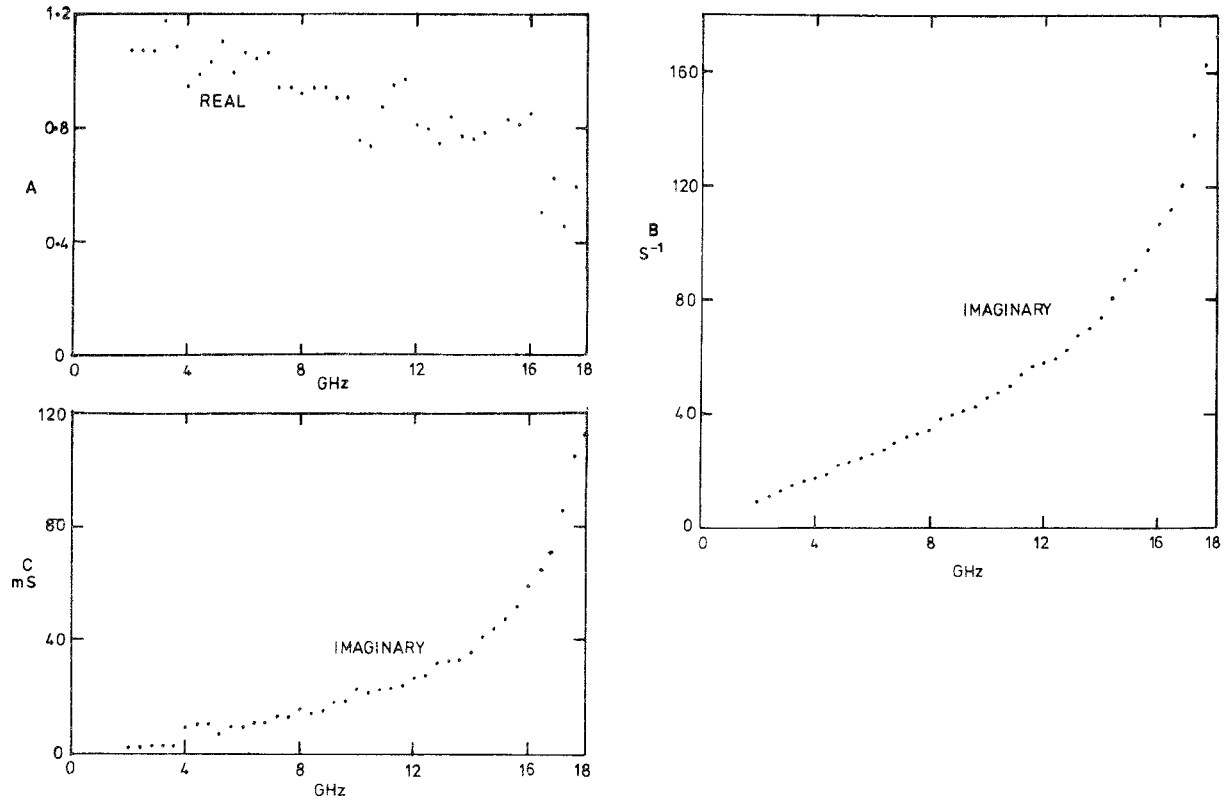

Fig. 9. Package characterization for device number 1978 in 50-Ω coaxial mount of Fig. 1.

Both real and imaginary parts of A, B, and C are plotted against frequency in Fig. 8. If the package and mount had been totally lossless, then A would be real, B imaginary, and C imaginary. The imaginary part of A and the real parts of B and C, therefore, represent the mounted package losses. It can be seen that these losses increase with frequency as expected (due, for instance, to the skin effect in the bond wire). However, the losses are small and do not have a significant effect upon the computation of device admittances [13]. The losses are neglected in Fig. 9.

Note that no attempt has been made to smooth the results plotted in Figs. 8 and 9. Nevertheless, results for B and C lie on a fairly smooth curve, although the results for A tend to fluctuate rather more. This is due mainly to systematic errors in the network analyzer. The situation could be improved by taking measurements over a smaller frequency range because this would effect an improvement in network analyzer calibration and tracking accuracy.

As previously shown in Fig. 1, the characterizations presented are for the S4 package in a 50-Ω 7-mm airline mount. If an alternative mount were to be used (e.g., different impedance line or different line dimensions), then the characterization would also be different.

Finally, it should be noted that although the characterizations for the two device packages follow the same basic trends, there are significant differences between them. This was to be expected from the discussion in Section II-A regarding production tolerances and other variables.

B. Error Estimation and Correction

In Section III-A, it was shown that three sets of passive admittance measurements together with three measured device conductances were sufficient to characterize the microwave circuit surrounding the device. Two characterizations, typical of several obtained, were presented in Section IV-A.

A simple method is now presented by which the accuracy of the characterization may be assessed. It entails taking a fourth set of passive measurements (Y_{M4}, G_{04}) from which the terminal admittance may be computed, using (8), as

$$Y_{D4} = \frac{A - BY_{M4}}{CY_{M4} - 1}. \tag{24}$$

Now, if the initial characterization was accurate (i.e., if A, B, and C were accurately evaluated), we should have

$$Y_{D4} = G_{04} + j\omega C_0 \tag{25}$$

where G_{04} and C_0 have been independently evaluated by dc measurement and estimation, respectively.

It is apparent that, in the absence of characterization error, the value of Y_{D4} obtained from (24) would have a real part that is constant and equal to G_{04} and an imaginary part that increases with frequency with a constant gradient equal to C_0.

The results of performing such an exercise on the diodes used in Section IV-A are shown in Fig. 10. The plotted points (which are unsmoothed) are the device admittance Y_{D4} derived from a fourth set of measure-

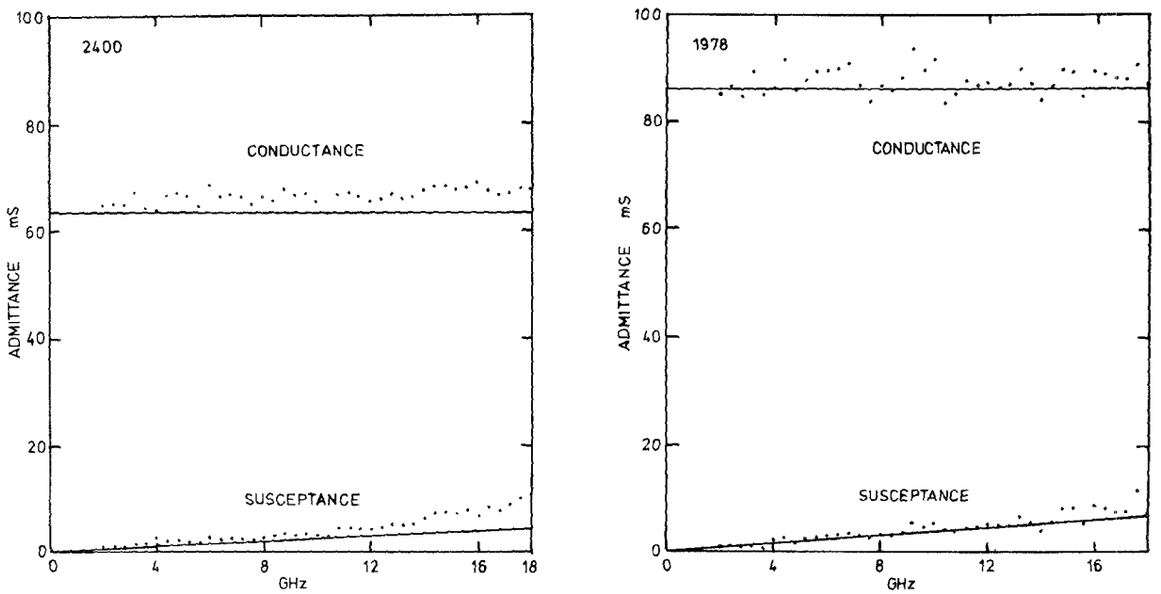

Fig. 10. Comparison of computed passive device admittance Y_{D4} (plotted points) with actual device admittance $G_{04}+j\omega C_{04}$ (straight lines) for device numbers 2400 and 1978. Y_{D4} is computed from measured admittance Y_{M4} using characterization results (A, B, C) of Figs. 8 and 9.

ments Y_{M4} which were taken at a magnetic field of approximately 1 T. G_{04} was measured as 63.3 and 86.1 ms for device numbers 2400 and 1978, respectively, and is drawn as a straight line in the graphs. The estimated device susceptance (C_0 estimated as 0.04 and 0.06 pF for device numbers 2400 and 1978, respectively) is also drawn as a straight line.

It can be seen that there is generally good agreement between the plotted points and the straight lines, although the values of G_{D4} appear, on average, to be slightly greater than G_{04} for both devices. (The error for device 1978 is less than 3 percent and for device 2400 less than 5 percent.) Also, the estimated capacitance for device 2400 appears to be slightly too low (less than 10-percent error below 12 GHz, but rising considerably at higher frequencies).

These discrepancies indicate small but significant errors in the original characterization. However, they also suggest that an iterative correction procedure may be possible whereby, for instance, the estimated value of C_0 may be adjusted (followed by recomputation of A, B, and C) until the discrepancies in Fig. 10 are minimized. Alternatively, if the principal source of error is known to be the frequency dependent substrate resistance, then it may be incorporated easily in the values of $G_{01}-G_{04}$ by reference to (23) in Section III-C.

C. Package Modeling: A Comparison of Dummy Package Results with Present Results

In order to compare the present S4 package characterization results with the admittance results of Owens [9], it is necessary to manipulate them so that they are in the same form. As pointed out in Section II-A, the technique adopted by Owens involves the measurement of short- and open-circuit package admittances, whereas the galvanomagnetic technique gives the three package admittance parameters A, B, and C.

By reference to (4) it may be seen, however, that short- and open-circuit package admittances (Y_D approaching infinity and equal to zero, respectively) are given by

$$Y_{S/C} = \frac{1}{B} \tag{26}$$

$$Y_{O/C} = \frac{C}{A}. \tag{27}$$

Moreover, these are true short- and open-circuit admittances because the internal geometry of the package has not been tampered with as in the dummy package technique.

The short- and open-circuit package admittances are plotted in Fig. 11 for the two characterizations given in Figs. 8 and 9. Only the lossless (susceptive) components are plotted because Owens' model assumes a lossless package. (In fact, the loss is very small.) The open- and short-circuit responses of Owens' equivalent circuit (Fig. 2), which represent the respective average values of four short-circuit and four open-circuit dummy package admittance measurements in the range 4–23.5 GHz, are drawn as continuous lines in Fig. 11.

Concentrating first on the short-circuit package admittances, it can be seen that there are significant differences between the average dummy package curve and the present results. The former has a resonant frequency of 20 GHz whereas, by extrapolation, the latter appear to be resonant at approximately 21 and 22 GHz.

Turning to the open-circuit admittances, it is evident that a considerable variation exists between Owens' results which show a resonance at approximately 15 GHz and the

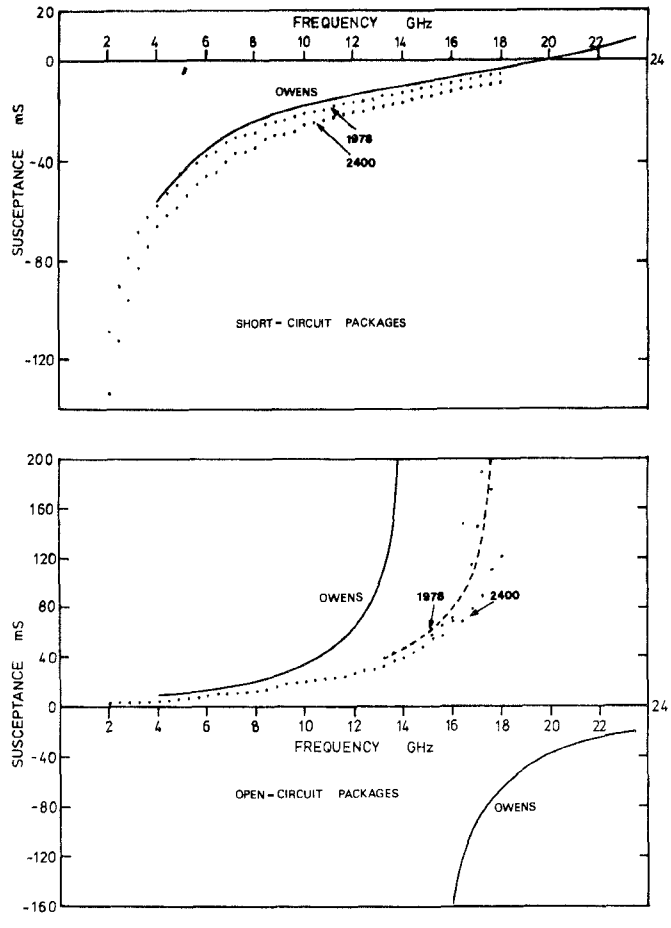

Fig. 11. Comparison of mounted S4 package admittances of Owens [9] (solid curves based on mean dummy package measurements) with similarly mounted S4 package admittances of device number 2400 and device number 1978 derived using the characterizations of Figs. 8 and 9, respectively.

present results which may be shown by extrapolation to resonate between approximately 18 and 21 GHz. The reason for the much lower resonant frequency of Owens' results is not readily apparent. It cannot, for instance, be attributed to differences in bond wire diameter because the dummy packages used a single loop of 50×10^{-6}-m diameter gold wire [6], whereas the present devices have a single loop of 25×10^{-6}-m gold wire which would have a larger inductance (assuming approximately equal lengths) and thus tend to give rise to lower resonant frequencies. The most likely explanation for the gross differences in the open-circuit resonant frequencies lies in the method of construction of the open-circuit dummy packages (described in Section II-A) in which a significant unwanted capacitance may have been contributed by the solid dielectric used to support the bond wire. It is interesting to note that an earlier paper [6] reported even lower short- and open-circuit resonant frequencies.

From the results presented above, it is evident that serious errors are associated with the use of dummy packages which cast considerable doubts over the applicability of that approach to device characterization and package modeling.

V. Conclusions

A galvanomagnetic technique has been presented which permits the characterization of stable transferred electron devices. The use of dummy packages is avoided, and, indeed, the microwave circuit remains physically undisturbed throughout the entire measurement procedure. Device characterization results have not been presented here but are to be presented in another paper in which they are compared with theory.

It was shown that relaxation effects are negligible, and that the skin effect resistance in the substrate of a typical low-power device also has a negligible effect upon the accuracy of the results. Providing that the device capacitance is estimated with sufficient accuracy, the remaining errors are mainly random fluctuations due to network analyzer measurement inaccuracies. As such, these are not serious and may be largely eliminated by a suitable smoothing procedure. One source of network analyzer inaccuracy was tracking error which could have been reduced by choosing a smaller frequency range or, better still, employing a low-noise microwave frequency synthesizer in place of the four conventional oscillators used to cover the band 2–18 GHz.

An extension of the basic technique to permit the characterization of transferred electron oscillators was proposed which, although experimentally untested, should be successful, provided that the device and circuit impedance may be chosen to allow an accurate passive characterization to be obtained.

The galvanomagnetic technique readily lends itself to automation because the automatic network analyzer depends, for its control, calibration, and correction sequence, on a minicomputer or microprocessor which (in conjunction with remotely programmable instruments) could be programmed to control the magnetic field, measure the device resistance, control the device bias, and, after completion of measurements, compute the circuit characterization followed by the active device admittance. A routine would also be incorporated to smooth the results.

The galvanomagnetic technique may find an important application in the characterization of transferred electron devices in microstrip circuits, which are being increasingly used as small low-cost microwave reflection amplifiers. Such circuits, which are often difficult to design accurately, usually employ unpackaged devices which are sometimes passivated with silicon rubber compounds. Characterization by the dummy package approach would thus be impossible, but the circuit arrangement is ideally suited to the galvanomagnetic technique.

Finally, short- and open-circuit package admittances were derived from the package characterization results and compared with the previous results obtained using dummy packages. It was shown that the use of dummy packages can give rise to serious errors which lead to the derivation of a grossly inaccurate equivalent circuit. Although, as expected, the galvanomagnetic technique reveals variations in the admittances of different

packages, these are relatively small. Therefore, it would be a useful exercise to derive a lumped element equivalent circuit (based on the average of the results obtained using the galvanomagnetic technique), possibly consisting of a ladder type of structure.

References

[1] K. Kurokawa, "Some basic characteristics of broadband negative resistance oscillator circuits," *Bell Syst. Tech. J.*, vol. 48, pp. 1937–1955, 1969.

[2] M. L. Jeremy, "Circuit characterization and noise properties of solid-state microwave oscillators," Ph.D. dissertation, Elec. and Electron. Eng. Dep., Univ. of Leeds, Leeds, England, 1975.

[3] J. W. Monroe, "The effects of package parasitics on the stability of microwave negative resistance devices," *IEEE Trans. Microwave Theory Tech.*, vol. MTT-21, pp. 731–735, 1973.

[4] B. S. Perlman, C. L. Upadhyayula, and R. E. Marx, "Wide-band reflection-type transferred electron amplifiers," *IEEE Trans. Microwave Theory Tech.*, vol. MTT-18, pp. 911–921, 1970.

[5] W. J. Getsinger, "The packaged and mounted diode as a microwave circuit," *IEEE Trans. Microwave Theory Tech.*, vol. MTT-14, pp. 58–69, 1966.

[6] R. P. Owens and D. Cawsey, "Microwave equivalent-circuit parameters of Gunn-effect-device packages," *IEEE Trans. Microwave Theory Tech.*, vol. MTT-18, pp. 790–798, 1970.

[7] I. W. Pence and P. J. Khan, "Broad-band equivalent circuit determination of Gunn diodes," *IEEE Trans. Microwave Theory Tech.*, vol. MTT-18, pp. 784–789, 1970.

[8] J. Roe and F. J. Rosenbaum, "Characterization of packaged microwave diodes in reduced height waveguide," *IEEE Trans. Microwave Theory Tech.*, vol. MTT-18, pp. 638–642, 1970.

[9] R. P. Owens, "Mount-independent equivalent circuit of the S4 diode package," *Electron. Lett.*, vol. 7, pp. 580–582, 1971.

[10] M. J. Howes and M. L. Jeremy, "Transferred-electron oscillator device plane measurements," *IEEE Trans. Electron Devices*, vol. ED-20, pp. 657–659, 1973.

[11] ——, "Large signal circuit characterization of solid/state microwave oscillator devices," *IEEE Trans. Electron Devices*, vol. ED-21, pp. 488–499, 1974.

[12] R. D. Pollard, M. J. Howes, and D. V. Morgan, "Design of Baritt oscillators based on large-signal measurements," in *Proc. 4th European Microwave Conf.*, Montreux, Switzerland, pp. 192–196, 1974.

[13] J. McBretney, "Galvanomagnetic phenomena in transferred electron devices," Ph.D. dissertation, Univ. of Leeds, Leeds, England, July 1977.

[14] H. D. Rees, "Time response of the high-field electron distribution function in GaAs," *IBM J. Res. Dev.*, vol. 13, pp. 537–542, 1970.

[15] Ramo *et al.*, *Fields and Waves in Communications Electronics*. New York: Wiley, 1965, p. 254 ff.

[16] G. W. Carter, *The Electromagnetic Field in its Engineering Aspects*. London, England: Longmans, 1967, ch. 11.

[17] F. A. Myers, "Gunn effect technology, part 1," *Microwave Syst. News*, vol. 5, pp. 67–71, Apr./May 1975.

Tapered Block Coupling and Mode Conversion in Integrated Optics

G. A. TEH, V. C. Y. SO, AND G. I. STEGEMAN

Abstract—**High-efficiency power transfer between two planar waveguides on separate substrates has been achieved via the tapered velocity mechanism. The method is simple and easily repeatable. The same setup can also be used as a mode converter as well as a mode filter.**

THE CURRENT EFFORT in integrated optics has resulted in numerous discrete thin-film devices [1]. The original aim [2] was to have all the components on a single substrate in the form of an integrated optical circuit. While such a development would no doubt be highly desirable, it may be some years before the objective is realized. In the meantime, a quasi-integrated optical system can still be obtained by interconnecting the various devices using couplers [1], [3], [4]. The tapered block coupler is proposed to serve such a function.

A tapered optical directional coupler with close to 100-percent coupling efficiency has been demonstrated in a multilayer structure [5]. Theory shows that this type of coupler has greatly improved tolerance properties and does not, in particular, suffer from the severe tolerance restriction placed on velocity synchronism in conventional uniform couplers. Hsu and Chang [3] introduced the concept of block coupling between two near-identical thin films on different substrates. Transfer efficiencies of up to 70 percent were obtained by cutting a single waveguide in half and pressing the two surfaces together. The 70-percent coupling efficiency is limited by phase mismatch [3]. A grating has also been used to exchange energy between

Manuscript received May 8, 1978; revised September 28, 1978. This research was supported by the Department of Communications, Ottawa, Ont., Canada.

G. A. Teh is with the Department of Physics, University of Toronto, Toronto, Ont., Canada, on leave from Nanyang University, Singapore.

V. C. Y. So and G. I. Stegeman are with the Department of Physics, University of Toronto, Toronto, Ont., Canada.

0018-9480/79/0300-0265$00.75 ©1979 IEEE